ACS OMEGA

Article

Cite This: ACS Omega 2019, 4, 3469−3475

http://pubs.acs.org/journal/acsodf

Comparison of K-*Ras* and N-*Ras* Mutagenic Hot Spots for UVC Damage

Sindhu G. Nair[†] and Glen R. Loppnow*[,†]

[†]Department of Chemistry, University of Alberta, Edmonton, Alberta T6G 2G2, Canada

Supporting Information

ABSTRACT: It has been well established that mutations in K-*Ras* and N-*Ras* proto-oncogenes can convert them into active oncogenes. Current molecular cancer research has been focused on determining the key steps by which cellular genes become oncogenes and not on the underlying and fundamental chemical damage mechanism and susceptibility to damage. In this study, we investigate the damage hot spots present in the N-*Ras* and K-*Ras* genes upon exposure to UVC radiation. Detection of damage is accomplished by a simple, sensitive, mix-and-read assay using an EvaGreen probe in a 96-well microtiter plate. Our results show that, although there is high degree of sequential similarities among K-*Ras* and N-*Ras* genes, they show different degrees of UV damage in different portions of their genomes. Our experiments demonstrate that overall, the K-*Ras* genome is more prone to UVC damage than the N-*Ras* genome. We observe that the extent of damage increases with increasing number of TTs in a sequence, consistent with previous results that show that thymine cyclobutyl photodimers are the primary DNA damage photoproducts upon UVC irradiation. This understanding of the effect of UVC radiation on various codons of K-*Ras* and N-*Ras* genes will help to increase our understanding about hot spots of DNA damage and the chemical damage mechanism.

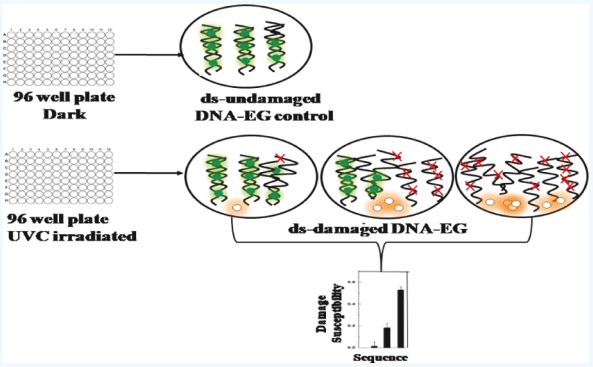

INTRODUCTION

Mutational activation of the *Ras* family of genes has been found to be one of the principal oncogenic events in cancer.[1,2] The *Ras* family encodes small GTPase proteins involved in cellular signal transduction and consist of three proto-oncogenes, K-*Ras*, N-*Ras*, and H-*Ras*.[1,3,4] Although there is a high degree of homogeneity among the different *Ras* gene sequences, preliminary studies have demonstrated that many different tumors are identified with different *Ras* genes.[5] However, no correlation has been established between an activated *Ras* oncogene and the tumor type present. Apparently, mutation of *Ras* proto-oncogenes is not essential for tumorigenesis, but it can still be a contributing factor to human carcinogenesis.[6]

Much effort has been made to investigate how mutation leads to the activation of the *Ras* genes. Past research has shown that mutation at any of the codons 12, 13, and 61 in any of the three *Ras* genes is capable of activating their oncogenic functions.[3,7,8] Interestingly, it has been found that mutation preferentially occurs at codon 12 of K-*Ras* rather than at codon 13 or 61 of K-*Ras* or at any N-*Ras* or H-*Ras* condon.[7,9,10] Furthermore, on investigating the repair mechanism between codon 12 and the other condons, it was observed that there was no substantial difference in their repair rates. These findings raise a pivotal question: What factors determine the oncogenic properties of *Ras* proto-oncogenes? In this paper, we explore one aspect of this question, the relationship between DNA damage and mutational hot spots of *Ras* genes.

It is well known that UV radiation is one of the major causes of skin cancer.[11] Animal model studies[12,13] have inferred that UV irradiation can introduce point mutations in the *Ras* proto-oncogene. These point mutations lead to the production of *Ras* protein with diminished or no GTPase activity. Loss of GTPase activity shifts the equilibrium between active GTP-bound *Ras* protein and inactive GDP-bound *Ras* protein to produce a more active GTP. The active GTP-bound *Ras* protein can now stimulate a plethora of downstream processes causing unregulated signal transduction and facilitating the development of skin cancer.[8,14−16] The major photoproducts induced in DNA by UVC light are the cyclobutyl pyrimidine photodimers (CPDs) and (6−4) pyrimidine-pyrimidinone photoproducts.[13,17] In vitro UVC irradiation experimental studies have already shown that UV light forms a point mutation at codons 12 and 61[8] in the N-*Ras* gene. Another site-directed mutagenesis experiment performed by introducing CPDs at predetermined sites showed that the photodimer could induce a point mutation at the modified positions.[18] However, it is equally important to determine if the *Ras* genes are activated by the production of CPD in the gene. Recent in

Received: October 30, 2018
Accepted: February 1, 2019
Published: February 15, 2019

DOI: 10.1021/acsomega.8b03017
ACS Omega 2019, 4, 3469−3475

Table 1. K-*Ras* and N-*Ras* Sequences Used in This Study[a]

K-*Ras*		N-*Ras*	
name	sequence	name	sequence
S_{1-7}	5′-ATG ACT GAA TAT AAA CTT GTG-3′	S_{1-7}	5′-ATG ACT GAG TAC AAA CTG GTG-3′
S_{7-13}	5′-GTG GTA GTT GGA GCT GGT GGC-3′	S_{7-13}	5′-GTG GTG GTT GGA GCA GGT GGT-3′
S_{13-19}	5′-GGC GTA GGC AAG AGT GCC TTG-3′	S_{13-19}	5′-GGT GTT GGG AAA AGC GCA CTG-3′
S_{19-25}	5′-TTG ACG ATA CAG CTA ATT CAG-3′	S_{19-25}	5′-CTG ACA ATC CAG CTA ATC CAG-3′
S_{25-31}	5′-CAG AAT CAT TTT GTG GAC GAA-3′	S_{25-31}	5′-CAG AAC CAC TTT GTA GAT GAA-3′
S_{31-37}	5′-GAA TAT GAT CCA ACA ATA GAG-3′	S_{31-37}	5′-GAA TAT GAT CCC ACC ATA GAG-3′
S_{37-43}	5′-GAG GAT TCC TAC AGG AAG CAA-3′	S_{37-43}	5′-GAG GAT TCT TAC AGA AAA CAA-3′
S_{43-49}	5′-CAA GTA GTA ATT GAT GGA GAA-3′	S_{43-49}	5′-CAA GTG GTT ATA GAT GGT GAA-3′
S_{49-55}	5′-GAA ACC TGT CTC TTG GAT ATT-3′	S_{49-55}	5′-GAA ACC TGT TTG TTG GAC ATA-3′
S_{55-61}	5′-ATT CTC GAC ACA GCA GGT CAA-3′	S_{55-61}	5′-ATA CTG GAT ACA GCT GGA CAA-3′
S_{61-67}	5′-CAA GAG GAG TAC AGT GCA ATG-3′	S_{61-67}	5′-CAA GAA GAG TAC AGT GCC ATG-3′
S_{67-73}	5′-ATG AGG GAC CAG TAC ATG AGG-3′	S_{67-73}	5′-ATG AGA GAC CAA TAC ATG AGG-3′
S_{73-79}	5′-AGG ACT GGG GAG GGC TTT CTT-3′	S_{73-79}	5′-AGG ACA GGC GAA GGC TTC CTC-3′
S_{79-85}	5′-CTT TGT GTA TTT GCC ATA AAT-3′	S_{79-85}	5′-CTC TGT GTA TTT GCC ATC AAT-3′
S_{85-91}	5′-AAT AAT ACT AAA TCA TTT GAA-3′	S_{85-91}	5′-AAT AAT AGC AAG TCA TTT GCG-3′
S_{91-97}	5′-GAA GAT ATT CAC CAT TAT AGA-3′	S_{91-97}	5′-GCG GAT ATT AAC CTC TAC AGG-3′
S_{97-103}	5′-AGA GAA CAA ATT AAA AGA GTT-3′	S_{97-103}	5′-AGG GAG CAG ATT AAG CGA GTA-3′
$S_{103-109}$	5′-GTT AAG GAC TCT GAA GAT GTA-3′	$S_{103-109}$	5′-GTA AAA GAC TCG GAT GAT GTA-3′
$S_{109-115}$	5′-GTA CCT ATG GTC CTA GTA GGA-3′	$S_{109-115}$	5′-GTA CCT ATG GTG CTA GTG GGA-3′
$S_{115-121}$	5′-GGA AAT AAA TGT GAT TTG CCT-3′	$S_{115-121}$	5′-GGA AAC AAG TGT GAT TTG CCA-3′
$S_{121-127}$	5′-CCT TCT AGA ACA GTA GAC ACA-3′	$S_{121-127}$	5′-CCA ACA AGG ACA GTT GAT ACA-3′
$S_{127-133}$	5′-ACA AAA CAG GCT CAG GAC TTA3′	$S_{127-133}$	5′-ACA AAA CAA GCC CAC GAA CTG-3′
$S_{133-139}$	5′-TTA GCA AGA AGT TAT GGA ATT-3′	$S_{133-139}$	5′-CTG GCC AAG AGT TAC GGG ATT-3′
$S_{139-145}$	5′-ATT CCT TTT ATT GAA ACA TCA-3′	$S_{139-145}$	5′-ATT CCA TTC ATT GAA ACC TCA-3′
$S_{145-151}$	5′-TCA GCA AAG ACA AGA CAG GGT-3′	$S_{145-151}$	5′-TCA GCC AAG ACC AGA CAG GGT-3′
$S_{151-157}$	5′-GGT GTT GAT GAT GCC TTC TAT-3′	$S_{151-157}$	5′-GGT GTT GAA GAT GCT TTT TAC-3′
$S_{157-163}$	5′-TAT ACA TTA GTT CGA GAA ATT-3′	$S_{157-163}$	5′-TAC ACA CTG GTA AGA GAA ATA-3′
$S_{163-169}$	5′-ATT CGA AAA CAT AAA GAA AAG-3′	$S_{163-169}$	5′-ATA CGC CAG TAC CGA ATG AAA-3′
$S_{169-175}$	5′-AAG ATG AGC AAA GAT GGT AAA-3′	$S_{169-175}$	5′-AAA AAA CTC AAC AGC AGT GAT-3′
$S_{175-181}$	5′-AAA AAG AAG AAA AAG AAG TCA-3′	$S_{175-181}$	5′-GAT GAT GGG ACT CAG GGT TGT-3′
$S_{181-187}$	5′-TCA AAG ACA AAG TGT GTA ATT-3′	$S_{181-187}$	5′-TGT ATG GGA TTG CCA TGT GTG-3′
$S_{183-189}$	5′-ACA AAG TGT GTA ATT ATG TAA-3′	$S_{184-190}$	5′-TTG CCA TGT GTG GTG ATG TAA-3′

[a]Oligonucleotide sequences for K-*Ras* and N-*Ras* genes are listed. The subscripts in the "Name" column denote the start and end codon numbers. Note that the first and last codons in each sequence overlap those on the previous and following strands, respectively. However, the last sequence for K-*Ras* has 5 and N-*Ras* has 4 overlapping codons from the previous strands. This is done to maintain a constant sequence length of 21 nucleobases. All the sequences listed above were annealed with their complementary sequences to form their respective dsDNA oligonucleotide.

vitro experiments have demonstrated that proto-oncogene expression in human epidermis increases as a result of UV radiation, leading to a high rate of cell proliferation and differentiation.[19]

Current molecular cancer research has been focused on determining the key steps by which cellular genes become oncogenes, not on the underlying and fundamental chemical damage mechanisms and susceptibility to damage. To address this, there is a need to develop a new assay that can screen the entire genome of DNA in a high-throughput fashion with nucleotide resolution. Microarray technology is being extensively used for the study of gene expression and its changes in different cell states for a large population of genes simultaneously.[20,21] However, the wider acceptance of the microarray is limited due to the use of time-consuming and potentially biased image processing software[22] for sample analysis. A DNA hybridization assay combined with fluorescence detection by label-free probes serves to be a simple, fast, inexpensive and sensitive method to study DNA damage.[23,24] Unlike the microarray, hybridization assays neither use laborious software for data analysis nor expensive fluorescently labeled DNA probes for damage quantification. In this work, we use a 96-well microplate platform coupled with a fluorescent intercalating dye, EvaGreen (EG),[25,26] to develop a multiplexed solution-phase hybridization assay for investigating the mutational hot spots of damage present in *Ras* genes. Earlier studies have already proven that K-*Ras* is more susceptible to mutation when compared to N-*Ras*.[3,15,27] Thus, in this study, we chose to investigate the effect of UVC radiation on the entire genomes of both K-*Ras* and N-*Ras*.

RESULTS AND DISCUSSION

K-*Ras* and N-*Ras* Damage by UVC Radiation. The oligonucleotide sequences used in this study that make up the K-*Ras* and N-*Ras* genes are listed in Table 1. To enable better localization of damage and to attempt to correlate damage susceptibility with sequence, each *Ras* gene was split into 32 oligonucleotide sequences of 7 codons each, with the first and last codons in each sequence overlapping in the previous and following sequences, respectively. All oligonucleotides for both *Ras* genes gave a positive damage response to UVC radiation, i.e., all oligonucleotides showed a decrease in fluorescence from the EG dye upon increasing UVC irradiation. EG dye is an intercalating dye constructed of two monomeric units

DOI: 10.1021/acsomega.8b03017
ACS Omega 2019, 4, 3469−3475

joined through a flexible linker. This dimeric dye is inactive in the absence of dsDNA and assumes a closed-looped conformation in a solution with two chromophores in close proximity to one another. In this conformation, the fluorescence is quenched. This looped conformation of EG opens upon binding and intercalation to dsDNA when present, separating the two chromophores. In this open, intercalated form, the EG exhibits maximum fluorescence. The equilibrium between the inactive and active form of EG in the presence of DNA is regulated by the DNA double helical structure. Upon damage of dsDNA, a change in its helical structure occurs due to the disruptions to the normal base paring, leading to a release of bound EG and a consequent reduction in EG fluorescence.[25] Thus, we see a decrease in the fluorescence intensity with increasing damage (damage susceptibility). Damage susceptibility increases from 0 to 83% for K-*Ras* and 0−69% for N-*Ras*, depending on the nucleobases present in different sequences. The results of UVC-induced damage are listed in Table 2 for K-*Ras* and Table 3 for N-*Ras* oligonucleotide sequences.

To understand the relationship between UVC damage and the sequence composition, we plotted the correlation diagrams for all possible nucleobase pairs. Here it is worth mentioning that only the correlation depicted in Figure 1 shows a significant positive correlation of all the correlations between sequence and damage susceptibility attempted; all other plots are included in the Supporting Information (Figures S1 and S2) for completeness. Figure 1 indicates the plot with damage susceptibility as a function of number of TT sites for both K-*Ras* and N-*Ras* oligonucleotide sequences. It is already known that DNA damage by UVC radiation primarily occurs due to the formation of pyrimidine dimers such as cyclobutane pyrimidine dimers (CPDs), [6−4] pyrimidine pyrimidinone photoproducts ([6−4] PPs), and photohydrates.[28,29] The CPDs and [6−4] PPs can potentially be formed between TT, CC, CT, and TC[30] nucleotide pairs. From Figure 1, it can be clearly seen that the damage shows a strong positive linear correlation with increasing numbers of TT sites; no significant correlation is seen between damage and other bipyrimidine sites (see the Supporting Information). This result is expected for UVC-induced dsDNA damage, since the yield of T<>T photodimers is the highest (~77%) compared to any other bipyrimidine lesion.[31−33] It is interesting that the UVC-induced dsDNA damage gives a better R^2 value for K-*Ras* (0.90) than for N-*Ras* (0.23) oligonucleotides. This could be because of the presence of a higher total number (134) and larger range (0−10) of TT sites in K-*Ras* when compared to the number (93) and range (0−6) of TT sites in N-*Ras* oligonucleotides. Another interesting result obtained by the study of damage susceptibility as a function of sequence composition is a small, negative correlation between damage and GG (R^2 = 0.44) or GT (R^2 = 0.35) bipyrimidine sites in K-*Ras* (Figures S1 and S2), suggesting that GG and GT bipyrimidine sites may provide a mild protective effect to UVC irradiation. No such effect is observed in the N-*Ras* sequences.

The correlation between damage susceptibility and increasing number of TT sites in the K-*Ras* oligonucleotides deserves further comment. Although a statistically significant correlation is observed, there are some deviations from this behavior when sequences with the same number of TT sites are compared. For example, comparing oligonucleotide sequences $S_{85\text{-}91}$, $S_{139\text{-}145}$, and $S_{181\text{-}187}$ with 7 TT sites shows that sequence $S_{181\text{-}187}$ exhibits a much lower damage susceptibility than the other two and much lower than expected from the correlation. In fact, the damage susceptibility for $S_{181\text{-}187}$ is more closely consistent with the damage susceptibility for the closely related sequence $S_{183\text{-}189}$, which shares the last 5 condons with $S_{181\text{-}187}$. Furthermore, investigating sequences with 7 TT sites, we found that sequences that include a guanine adjacent to TT sites give lower damage susceptibility. In sequence-dependent studies on T<>T photodimer rates, Sarasin et al.[31] and Kohler et al.[33] have established that in tetrads of the type XTTY, the rate of dimer formation is higher for CTTC, TTTC, TTTA, TTTT, ATTC, CTTA, and ATTA and lower for GTTG, GTTC, GTTT, and GTTA. This model predicts, then, that all the tetrads with Gs adjacent to a TT site lower the rate of T<>T photodimer formation and that sequence $S_{181\text{-}187}$ with 2 GTTT tetrads would have lower damage susceptibility, which is what is observed.

Having established that the damage of K-*Ras* sequences by UVC irradiation appears to be related to T<>T photodimer formation, modulated by adjacent guanines, we now similarly analyze the N-*Ras* gene sequences. Table 3 shows the UVC-

Table 2. UVC-Induced Damage Susceptibility and Number of Bipyrimidine Sites of K-*Ras* Oligonucleotides[a]

sequence number	damage susceptibility	TT	CC	CT
$S_{175\text{-}181}$	0.83 ± 0.01	10	0	7
$S_{163\text{-}169}$	0.73 ± 0.02	9	0	4
$S_{97\text{-}103}$	0.80 ± 0.01	8	0	6
$S_{85\text{-}91}$	0.75 ± 0.01	7	0	3
$S_{139\text{-}145}$	0.72 ± 0.01	7	1	4
$S_{181\text{-}187}$	0.38 ± 0.02	7	0	4
$S_{133\text{-}139}$	0.62 ± 0.01	6	1	5
$S_{79\text{-}85}$	0.53 ± 0.02	6	1	1
$S_{115\text{-}121}$	0.48 ± 0.01	6	2	3
$S_{183\text{-}189}$	0.33 ± 0.02	6	0	1
$S_{157\text{-}163}$	0.46 ± 0.01	5	0	4
$S_{169\text{-}175}$	0.42 ± 0.02	5	1	4
$S_{25\text{-}31}$	0.43 ± 0.01	5	1	4
$S_{1\text{-}7}$	0.62 ± 0.01	4	0	4
$S_{127\text{-}133}$	0.40 ± 0.01	4	2	6
$S_{49\text{-}55}$	0.36 ± 0.02	4	1	7
$S_{43\text{-}49}$	0.20 ± 0.03	4	1	6
$S_{103\text{-}109}$	0.40 ± 0.01	3	1	8
$S_{91\text{-}97}$	0.32 ± 0.02	3	1	6
$S_{73\text{-}79}$	0.31 ± 0.05	3	6	7
$S_{37\text{-}43}$	0.24 ± 0.02	3	3	8
$S_{145\text{-}151}$	0.15 ± 0.02	3	2	7
$S_{31\text{-}37}$	0.12 ± 0.02	3	1	6
$S_{13\text{-}19}$	0.19 ± 0.03	2	3	5
$S_{151\text{-}157}$	0.16 ± 0.03	2	2	5
$S_{55\text{-}61}$	0.14 ± 0.02	2	1	7
$S_{61\text{-}67}$	0.14 ± 0.03	2	1	6
$S_{121\text{-}127}$	0.11 ± 0.01	2	1	7
$S_{19\text{-}25}$	0.00 ± 0.03	2	0	6
$S_{7\text{-}13}$	0.18 ± 0.02	1	4	4
$S_{67\text{-}73}$	0.01 ± 0.03	0	4	6
$S_{109\text{-}115}$	0.00 ± 0.01	0	4	6

[a]This table is ordered by the number of TT bipyrimidine sites in the K-*Ras* oligonucleotides used in this study. The damage susceptibility is calculated as $(1 - F)$, where $F = F_i/F_c$, F_i is the fluorescence intensity of EG-dsDNA upon damage and F_c is the fluorescence intensity of the undamaged DNA-EG control sample. The columns headed as "TT", "CC", and "CT" list the number of respective bipyrimidine sites in the oligonucleotides.

DOI: 10.1021/acsomega.8b03017
ACS Omega 2019, 4, 3469−3475

Table 3. UVC-Induced Damage Susceptibility and Number of Bipyrimidine Sites of N-*Ras* Oligonucleotides[a]

sequence number	damage susceptibility	TT	CC	CT
S_{37-43}	0.69 ± 0.02	6	1	4
$S_{151-157}$	0.53 ± 0.03	6	1	3
$S_{169-175}$	0.33 ± 0.02	6	0	5
$S_{139-145}$	0.69 ± 0.01	5	2	4
$S_{115-121}$	0.32 ± 0.01	5	2	3
S_{85-91}	0.26 ± 0.02	5	0	3
$S_{127-133}$	0.19 ± 0.00	5	2	3
S_{49-55}	0.18 ± 0.02	5	2	3
S_{13-19}	0.31 ± 0.01	4	3	1
S_{25-31}	0.23 ± 0.03	4	1	5
$S_{103-109}$	0.45 ± 0.02	3	1	5
$S_{133-139}$	0.30 ± 0.02	3	4	4
$S_{163-169}$	0.26 ± 0.01	3	2	3
$S_{157-163}$	0.23 ± 0.02	3	1	5
$S_{121-127}$	0.22 ± 0.01	3	2	4
S_{43-49}	0.21 ± 0.01	3	2	3
S_{79-85}	0.16 ± 0.03	3	1	2
S_{97-103}	0.41 ± 0.02	2	2	6
S_{91-97}	0.26 ± 0.00	2	3	4
S_{19-25}	0.19 ± 0.01	2	2	7
S_{73-79}	0.18 ± 0.03	2	4	8
$S_{184-190}$	0.13 ± 0.01	2	2	0
S_{61-67}	0.09 ± 0.01	2	1	5
S_{1-7}	0.12 ± 0.03	2	1	4
$S_{175-181}$	0.34 ± 0.02	1	4	6
S_{55-61}	0.10 ± 0.03	1	2	5
S_{31-37}	0.01 ± 0.02	1	3	5
S_{7-13}	0.00 ± 0.02	1	5	2
S_{67-73}	0.00 ± 0.03	1	2	8
$S_{145-151}$	0.00 ± 0.02	1	4	5
$S_{181-187}$	0.00 ± 0.02	1	3	1
$S_{109-115}$	0.00 ± 0.03	0	4	4

[a]This table is ordered by the number of TT bipyrimidine sites in the N-*Ras* oligonucleotides used in this study. The damage susceptibility is calculated as $(1 - F)$, where $F = F_i/F_c$, F_i is the fluorescence intensity of EG-dsDNA upon damage and F_c is the fluorescence intensity of the undamaged DNA-EG control sample. The columns headed as TT, CC, and CT list the number of respective bipyrimidine sites in the oligonucleotides.

induced damage susceptibilities for the N-*Ras* sequences arranged in the order of decreasing number of TT sites. Here, we also see a general decrease in damage susceptibility with decreasing number of TT sites. However, we see a few more exceptions for N-*Ras* than for K-*Ras*, which will be discussed in detail.

On comparing sequences S_{37-43}, $S_{151-157}$, and $S_{169-175}$ with 6 TT sites, the damage susceptibility for sequence $S_{169-175}$ is much lower than that of the other two sequences with 6 TT sites. On correlating the damage to the neighboring nucleotides, no obvious justification could be established for this deviation. In addition, we investigated the position of TT sites for all the above sequences. We found that if the TT sites are distributed throughout the dsDNA, the T<>T photodimer formation will effectively destabilize the dsDNA more when compared to sequences with TT sites clustered more closely together. This effect of the distribution of TT site positions on the change in damage susceptibility is confirmed for sequence $S_{169-175}$, where all the 6 TT sites are located at the terminal and semiterminal positions[24] between nucleobase number 1 and

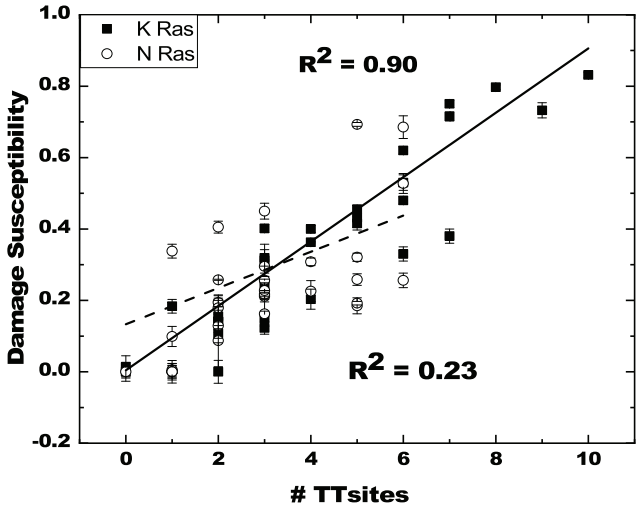

Figure 1. UVC damage susceptibility $(1 - F)$ as a function of the number of TT dinucleotide sites for K-*Ras* and N-*Ras*. The damage susceptibility on the *y*-axis is $1 - F$, where $F = F_i/F_c$, F_i is the fluorescence intensity of EG-dsDNA upon UVC damage and F_c is the fluorescence intensity of the undamaged DNA-EG control sample. The EG dye fluorescence intensity at 530 nm is measured in the presence of 1 μM dsDNA (10 mM Tris, 1 mM ethylenediaminetetraacetic acid (EDTA), 10 mM NaCl, pH 7.4). The solid line through the filled square points is a linear fit for the K-*Ras* sequences with its R^2 value indicated in the upper portion of the plot. The dashed line through the empty circle points is the linear fit for the N-*Ras* sequences with its R^2 value indicated in the lower portion of the plot.

11. Thus, hydrogen bonding between nucleobase number 12 to 21 of the dsDNA remains unperturbed, and this provides the required hydrophobic environment for EG to intercalate between the nucleobases of the second half of dsDNA, contributing to the higher fluorescence intensity. On the contrary, the 6 TT sites in oligonucleotide sequence S_{37-43} are randomly located at terminal, semiterminal, and central position of both the strands of the dsDNA. This distribution will destabilize the dsDNA structure throughout the entire 21 nucleobase sequence and give a higher damage susceptibility due to the presence of more nonfluorescent EG in solution. This result is in agreement with the earlier findings of the significant effect of mismatch position on DNA duplex stability.[24]

Furthermore, comparing the N-*Ras* sequences with 5 TT sites ($S_{139-145}$, $S_{115-121}$, S_{85-91}, $S_{127-133}$, and S_{49-55}), only sequence $S_{139-145}$ gives a high damage susceptibility (~60%) and all the other sequences exhibit a low damage susceptibility (20−30%). In these oligonucleotide sequences, the presence of neighboring Gs to the TT sites does account for the discrepancy in damage susceptibility. A detailed analysis shows that oligonucleotide sequences $S_{115-121}$ (0.32 ± 0.01) and S_{85-91} (0.26 ± 0.02) have GTTC tetrads and oligonucleotide sequence $S_{127-133}$ (0.19 ± 0.00) contains GTTT, GTTC, and CTTG tetrads. Similarly, oligonucleotide sequence S_{49-55} gives a low damage susceptibility of 0.18 ± 0.02 and contains GTTT and GTTG tetrads.

The above predictive model is further verified by comparing the olignucleotide sequence S_{85-91} of both K-*Ras* and N-*Ras*. These two sequences differ only in the neighboring nucleobases at 1 TT site out of the 4 TT sites present (excluding terminal TT sites with the least effect on the apparent damage susceptibility[24]). The tetrad ATTT in K-*Ras*

DOI: 10.1021/acsomega.8b03017
ACS Omega 2019, 4, 3469−3475

sequence is replaced by GTTC in N-*Ras*. Basically, replacing the adenosine of the K-*Ras* tetrad with guanosine in N-*Ras* tetrad drops the damage susceptibility of N-*Ras* by ∼3 times. Thus, the quenching effect of a neighboring G nucleobase can play a vital role in the T<>T photodimer formation rate and the subsequent damage susceptibility.[34,35]

These results for UVC-induced DNA damage in K-*Ras* and N-*Ras* sequences establishes an excellent agreement between damage and the effect of neighboring gaunine nucleobase on T<>T photodimer formation rate. This result is consistent with the sequence dependence of T<>T damage formation observed by Sarasin et al.[31] and Kohler et al.[33] In addition, the position of TT sites has been shown to account for the different damage susceptibilities of different K-*Ras* and N-*Ras* oligonucleotide sequences, as well as of the genes themselves.

A potential discrepancy in the trend of damage susceptibility is observed for sequences with 1−4 TT sites. With more than 4 TT sites, the formation of T<>T photodimers seems to dominate the damage susceptibility, as discussed above. However, greater deviations from the correlation are seen for oligonucleotide sequences with 4 or fewer TT sites. For example, oligonucleotide sequences $S_{1\text{-}7}$, $S_{49\text{-}55}$, and $S_{127\text{-}133}$ for K-*Ras* and $S_{97\text{-}103}$, $S_{103\text{-}109}$, and $S_{175\text{-}181}$ for N-*Ras* have 1−4 TT sites and show a damage susceptibility ranging between 30 and 65%. This could be due to the fact that UVC radiation damages other bipyrimidine sites, such as TC, CT, and CC, to some extent. The bipyrimidine dimer formation yields upon UVC radiation is reported to occur in the order TT > TC > CT > CC.[33] Thus, in the absence or presence of a low number of T<>T photodimer, there is a probability of forming other bipyrimidine photoproducts. Sequence $S_{1\text{-}7}$ of K-*Ras* with only 4 TT sites exhibits a damage susceptibility of 0.62 ± 0.01. This high damage susceptibility might be attributed to the presence of 4 TC/CT sites.

From Tables 2 and 3, it is clear that the damage susceptibility of most K-*Ras* oligonucleotide sequences is larger than their analogous N-*Ras* oligonucleotide sequence. Several biological studies performed on different tumor types have confirmed K-*Ras* genes to be more prone to mutation than N-*Ras* genes.[27] The COSMIC (the Catalog of Somatic Mutations in Cancer) data set confirms that 22% of K-*Ras* genes are mutated in comparison to 8% of N-*Ras* genes in all tumors analyzed.[3] Consistent with the biological results, our data give a larger damage susceptibility (∼83%) for K-*Ras* than for N-*Ras* (∼69%). This is mainly due to the presence of the higher number of TT sites in the K-*Ras* gene, making them more prone to DNA damage. However, the oligonucleotide sequences that correspond to the biologically active codons 12, 13, and 61 did not show any remarkable UVC damage susceptibility in either of the *Ras* genes. This result is not too surprising, since UVC irradiation may not be the primary insult to lead to oncogenic *Ras* genes. To understand the role of the biologically active codons of *Ras* genes in further detail, more research on the biological insults responsible for transforming the proto-oncogenes into oncogenes is required. However, we can use our method to further explore other types of DNA damage, such as oxidative and chemical damage, to gain further insight into the proto-oncogene formation mechanism.

CONCLUSIONS

The different mutagenic susceptibility of K-*Ras* and N-*Ras* genes has been shown here to correlate with molecular-level differences in UVC-induced damage susceptibility. Parallelizing a simple and rapid mix-and-read assay using EG dye as a fluorescence reporter and splitting the genes into shorter oligonucleotide sequences allow us to easily specify the cause of damage due to thymine−thymine cyclobutyl photodimers (CPDs), modulated by gaunosine residues on either side of the TT pairs within each codon.

EXPERIMENTAL SECTION

Materials. Oligonucleotide targets were obtained from Integrated DNA Technologies, Inc. (Coralville, IA). Hydrochloric acid was obtained from Anachemia (Montreal, QC, Canada), sodium chloride was obtained from ACP Chemical Inc. (Montreal, Quebec), Tris was obtained from ICN biomedicals (Aurora, OH), and ethylenediaminetetraacetic acid (EDTA) was obtained from BDH Inc. (Toronto, ON, Canada). The complete sequences of K-Ras and N-Ras genes are listed in Tables S1 and S2, respectively (see the Supporting Information). These genes are further subdivided into 32 overlapping sequences, with each sequence having a length of 21 nucleobases (Table 1).

DNA Damage Induced by UV Radiation. For DNA damage experiments, 147 μL of 1.36 μM nitrogen-purged dsDNA samples of each target sequence mentioned in Table 1 was placed in a separate well of a 96-well plate (Corning Special Optics, NY). UV light from UVC lamps emitting at 254 nm was chosen for irradiation. The UVC lamps in a Luzchem (Ottawa, ON, Canada) DEV photoreactor were turned on for 20 min prior to the experiment to ensure a stabilized light source. The photoreactor was purged continuously with nitrogen to remove oxygen and minimize ozone generation from the lamp. Finally, the 96-well microplate was placed in the photoreactor. Each well of the 96-well microplate was exposed to UVC light continuously for 2 h. Control samples were handled under identical condition, but were not exposed to UVC light and kept in the dark. After irradiation, the 96-well microplates were removed from the photoreactor and EG dye was added to each well. The final concentrations of the dsDNA and EG dye were a fixed ratio of 1:1.33.

Fluorescence Measurements. Room-temperature EvaGreen fluorescence intensities for UV-exposed dsDNA solutions were measured using a Safire fluorescence plate reader (Tecan, Mannendorf, Switzerland) after the addition of EG dye followed by incubation at 37 °C for 20 min in the dark. Fluorescence emission spectra were recorded using an excitation wavelength of 490 nm and an emission wavelength of 530 nm. The fluorescence spectra of dsDNA alone gave a minimum or zero background at the 530 nm emission wavelength.

ASSOCIATED CONTENT

Supporting Information

The Supporting Information is available free of charge on the ACS Publications website at DOI: 10.1021/acsomega.8b03017.

DNA damage susceptibility in the oligonucleotide sequences of Table 1 as a function of GG/CC, GA/CT, GT, and GC dinucleotides; N-Ras and K-Ras nucleotide sequences (PDF)

DOI: 10.1021/acsomega.8b03017
ACS Omega 2019, 4, 3469−3475

AUTHOR INFORMATION

Corresponding Author

*E-mail: glen.loppnow@ualberta.ca. Phone: (780) 492-9704. Fax: (780) 492-8231.

ORCID

Glen R. Loppnow: 0000-0002-4630-8663

Notes

The authors declare no competing financial interest.

ACKNOWLEDGMENTS

The authors acknowledge the financial support for this project from the Canadian Natural Sciences and Engineering Research Council (NSERC) Discovery Grants and the Faculty of Science, University of Alberta.

REFERENCES

(1) Jin, Y.; Shima, Y.; Furu, M.; Aoyama, T.; Nakamata, T.; Nakayama, T.; Nakamura, T.; Toguchida, J. Absence of oncogenic mutations of RAS family genes in soft tissue sarcomas of 100 Japanese patients. *Anticancer Res.* **2010**, *30*, 245−251.

(2) Ramdzan, Z. M.; Pal, R.; Vadnais, C.; Vandal, G.; Cadieux, C.; Leduy, L.; Davoudi, S.; Yao, L.; Karnezis, A. K.; Paquet, M.; Dankort, D.; Nepveu, A.; et al. RAS-Transformation in cancer cells require CUX1-dependent repair of oxidative DNA damage. *PLoS Biol.* **2014**, *12*, No. e1001807.

(3) Prior, I. A.; Lewis, P. D.; Mattos, C. A comprehensive survey of Ras mutations in cancer. *Cancer Res.* **2012**, *72*, 2457−2467.

(4) Macaluso, M.; Russo, G.; Cinti, C.; Basan, V.; Gebbia, N.; Russo, A. Ras family genes: An interesting link between cell cycle and cancer. *J. Cell Physiol.* **2002**, *192*, 125−130.

(5) To, M. D.; Rosario, R.; Westcott, P. M.; Banta, K. L.; Balmain, A. Interactions between wild-type and mutant Ras genes in lung and skin carcinogenesis. *Oncogene* **2013**, *32*, 4028−4033.

(6) Fernández-Medarde, A.; Santos, E. Ras in cancer and developmental diseases. *Genes Cancer* **2011**, *2*, 344−358.

(7) Feng, Z.; Hu, W.; Chen, J. X.; Pao, A.; Li, H.; Rom, W.; Hung, M. C.; Tang, M. S. Preferential DNA damage and poor repair determine ras gene mutational hotspot in human cancer. *J. Natl. Cancer Inst.* **2002**, *94*, 1527−1536.

(8) Pierceall, W. E.; Kripke, M. L.; Ananthaswamy, H. N. N-ras mutation in ultraviolet radiation-induced murine skin cancers. *Cancer Res.* **1992**, *52*, 3946−3951.

(9) Graziano, S. L.; Gamble, G. P.; Newman, N. B.; Abbott, L. Z.; Rooney, M.; Mookherjee, S.; Lamb, M. L.; Kohman, L. J.; Poiesz, B. J. Prognostic significance of K-ras codon 12 mutations in patients with resected stage I and II non-small-cell lung cancer. *J. Clin. Oncol.* **1999**, *17*, 668−675.

(10) Slebos, R. J.; Hruban, R. H.; Dalesio, O.; Mooi, W. J.; Offerhaus, G. J.; Rodenhuis, S. Relationship between K-ras oncogene activation and smoking in adenocarcinoma of the human lung. *J. Natl. Cancer Inst.* **1991**, *83*, 1024−1027.

(11) Glass, A. G.; Hoover, R. N. The emerging epidemic of melanoma and squamous cell skin cancer. *JAMA, J. Am. Med. Assoc.* **1989**, *262*, 2097−2100.

(12) Su, F.; Viros, A.; Milagre, C.; Trunzer, K.; Bollag, G.; Spleiss, O.; Reis-Filho, J. S.; Kong, X.; Koya, R. C.; Flaherty, K. T.; et al. RAS mutations in cutaneous squamous-cell carcinomas in patients treated with BRAF inhibitors. *N. Engl. J. Med.* **2012**, *366*, 207−215.

(13) Kamiya, H.; Murata, N.; Murata, T.; Iwai, S.; Matsukage, A.; Masutani, C.; Hanaoka, F.; Ohtsuka, E. Cyclobutane thymine dimers in a ras proto-oncogene hot spot activate the gene by point mutation. *Nucleic Acids Res.* **1993**, *21*, 2355−2361.

(14) Roddey, P. K.; Garmyn, M.; Park, H.; Bhawan, J.; Gilchrest, B. A. Ultraviolet irradiation induces c-fos but not c-Ha-ras proto-oncogene expression in human epidermis. *J. Invest. Dermatol.* **1994**, *102*, 296−299.

(15) Baines, A. T.; Xu, D.; Der, C. J. Inhibition of Ras for cancer treatment: the search continues. *Future Med. Chem.* **2011**, *3*, 1787−1808.

(16) Schubbert, S.; Zenker, M.; Rowe, S. L.; Böll, S.; Klein, C.; Bollag, G.; van der Burgt, I.; Musante, L.; Kalscheuer, V.; Wehner, L.; et al. Germline KRAS mutations cause Noonan syndrome. *Nat. Genet.* **2006**, *38*, 331−336.

(17) Climent, T.; González-Ramírez, I.; González-Luque, R.; Merchán, M.; Serrano-Andrés, L. Cyclobutane Pyrimidine Photodimerization of DNA/RNA Nucleobases in the Triplet State. *J. Phys. Chem. Lett.* **2010**, *1*, 2072−2076.

(18) Banerjee, S. K.; Borden, A.; Christensen, R. B.; LeClerc, J. E.; Lawrence, C. W. SOS-dependent replication past a single trans-syn T-T cyclobutane dimer gives a different mutation spectrum and increased error rate compared with replication past this lesion in uninduced cells. *J. Bacteriol.* **1990**, *172*, 2105−2112.

(19) Brenner, M.; Coelho, S. G.; Beer, J. Z.; Miller, S. A.; Wolber, R.; Smuda, C.; Hearing, V. J. Long-lasting molecular changes in human skin after repetitive in situ UV irradiation. *J. Invest. Dermatol.* **2009**, *129*, 1002−1011.

(20) Wei, H.; Kuan, P. F.; Tian, S.; Yang, C.; Nie, J.; Sengupta, S.; Ruotti, V.; Jonsdottir, G. A.; Keles, S.; Thomson, J. A.; Stewart, R. A study of the relationships between oligonucleotide properties and hybridization signal intensities from NimbleGen microarray datasets. *Nucleic Acids Res.* **2008**, *36*, 2926−2938.

(21) Powell, J.; Bennett, M.; Waters, R.; Reed, S. A novel global genome method to measure and map DNA damage: application for chemotherapy treatment stratification. *Lancet* **2014**, *383*, No. S83.

(22) Russo, G.; Zegar, C.; Giordano, A. Advantages and limitations of microarray technology in human cancer. *Oncogene* **2003**, *22*, 6497−6507.

(23) El-Yazbi, A. F.; Loppnow, G. R. Fluorescence of terbium ion-DNA complexes: a sensitive inexpensive probe for UV-induced DNA damage. *Anal. Chim. Acta* **2013**, *786*, 116−123.

(24) El-Yazbi, A. F.; Wong, A.; Loppnow, G. R. A luminescent probe of mismatched DNA hybridization: Location and number of mismatches. *Anal. Chim. Acta* **2017**, *994*, 92−99.

(25) El-Yazbi, A. F.; Loppnow, G. R. Probing DNA damage induced by common antiviral agents using multiple analytical techniques. *J. Pharm. Biomed. Anal.* **2018**, *157*, 226−234.

(26) Shoute, L. C. T.; Loppnow, G. R. Characterization of the binding interactions between EvaGreen dye and dsDNA. *Phys. Chem. Chem. Phys.* **2018**, *20*, 4772−4780.

(27) Johnson, L.; Mercer, K.; Greenbaum, D.; Bronson, R. T.; Crowley, D.; Tuveson, D. A.; Jacks, T. Somatic activation of the K-ras oncogene causes early onset lung cancer in mice. *Nature* **2001**, *410*, 1111−1116.

(28) Francesco, L.; Horspool, W. *CRC handbook of Organic Photochemistry and Photobiology*, 2nd ed.; CRC Press, 2003; pp 140.1−140.8.

(29) Ravanat, J. L.; Douki, T.; Cadet, J. Direct and indirect effects of UV radiation on DNA and its components. *J. Photochem. Photobiol., B* **2001**, *63*, 88−102.

(30) Zavala, A. G.; Morris, R. T.; Wyrick, J. J.; Smerdon, M. J. High-resolution characterization of CPD hotspot formation in human. *Nucleic Acid Res.* **2014**, *42*, 893−905.

(31) Bourre, F.; Renault, G.; Seawell, P. C.; Sarasin, A. Distribution of ultraviolet-induced lesions in Simian Virus 40 DNA. *Biochimie* **1985**, *67*, 293−299.

(32) Douki, T. Low ionic strength reduces cytosine photoreactivity in UVC-irradiated isolated DNA. *Photochem. Photobiol. Sci.* **2006**, *5*, 1045−1051.

(33) Law, Y. K.; Forties, R. A.; Liu, X.; Poirier, M. G.; Kohler, B. Sequence-dependent thymine dimer formation and photoreversal rates in double-stranded DNA. *Photochem. Photobiol. Sci.* **2013**, *12*, 1431−1439.

(34) Zheng, K. W.; Chen, Z.; Hao, Y. H.; Tan, Z. Molecular crowding creates an essential environment for the formation of stable

DOI: 10.1021/acsomega.8b03017
ACS Omega 2019, 4, 3469−3475

G-quadruplexes in long double-stranded DNA. *Nucleic Acids Res.* **2010**, *38*, 327−338.
(35) Kawanishi, S.; Hiraku, Y.; Oikawa, S. Mechanism of guanine-specific DNA damage by oxidative stress and its role in carcinogenesis and aging. *Mutat. Res., Rev. Mutat. Res.* **2001**, *488*, 65−76.

DOI: 10.1021/acsomega.8b03017
ACS Omega 2019, 4, 3469−3475